Spatial Heterogeneity Accompanying Gel Formation of Poly(N-isopropylacrylamide) Aqueous Solution at a Temperature below Cloud Point

Kogo, Takuro
Department of Applied Chemistry, Kyushu University

Shundo, Atsuomi
Department of Applied Chemistry, Kyushu University

Wang, Chi
Department of Chemical Engineering, National Cheng Kung University

Tanaka, Keiji
Department of Applied Chemistry, Kyushu University

出版情報：Macromolecules. 53 (24), pp.10964-10971, 2020-12-22. American Chemical Society
バージョン：

Spatial Heterogeneity Accompanying Gel Formation of Poly(*N*-isopropylacrylamide) Aqueous Solution at a Temperature below Cloud Point

Takuro Kogo,[a] Atsuomi Shundo,[a,b,c]* Chi Wang,[d]* and Keiji Tanaka[a,b,c,e]*

[a]*Department of Applied Chemistry, Kyushu University, Fukuoka 819-0395, Japan*

[b]*Department of Automotive Science, Kyushu University, Fukuoka 819-0395, Japan*

[c]*International Institute for Carbon-Neutral Energy Research (WPI-I2CNER), Kyushu University, Fukuoka 819-0395, Japan*

[d]*Department of Chemical Engineering, National Cheng Kung University, Tainan 701, Taiwan*

[e]*Center for Polymer Interface and Molecular Adhesion Science, Kyushu University, Fukuoka 819-0395, Japan*

*CORRESPONDING AUTHORS:

Tel: +81-92-802-2880 (A.S.), +886-6-2757575 ext 62645 (C.W.), +81-92-802-2878 (K.T.),

E-mails: a-shundo@cstf.kyushu-u.ac.jp (A.S.), chiwang@mail.ncku.edu.tw (C.W.), k-tanaka@cstf.kyushu-u.ac.jp (K.T.)

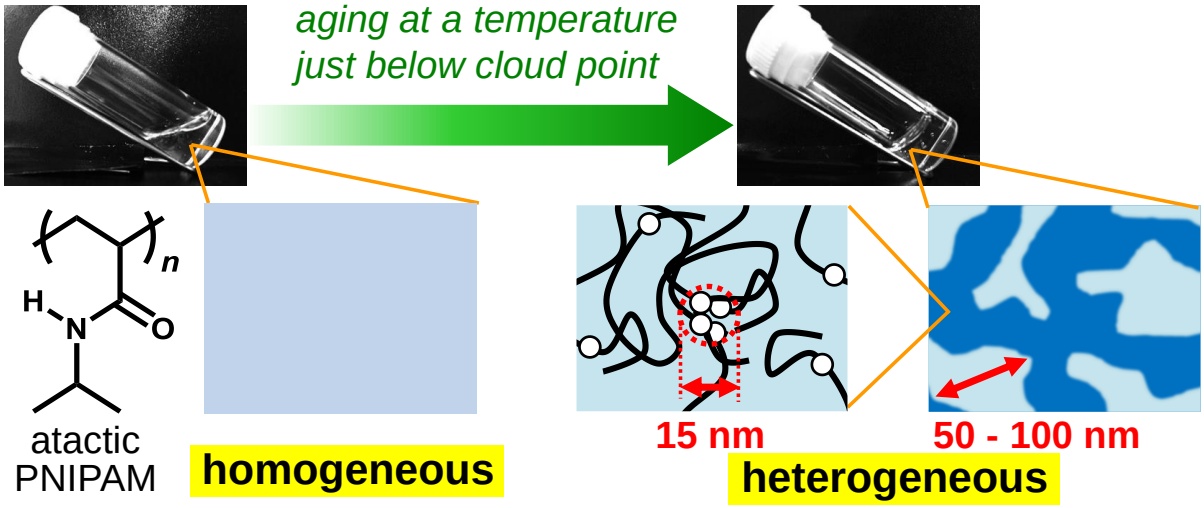
aging at a temperature
just below cloud point
n
H
N
O
atactic
PNIPAM
homogeneous
15 nm
50 - 100 nm
heterogeneous

ABSTRACT: Poly(*N*-isopropylacrylamide) (PNIPAM) is a representative thermoresponsive polymer and its aqueous solution becomes phase-separated at a temperature higher than the cloud point (T_{cp}) at ~304 K, which plays an important role in various biomedical applications. Thus, to further promote the use of PNIPAM as a functional material, it is necessary to gain a better understanding of its phase behavior especially at a temperature just below T_{cp}. To this end, we examined the local rheological properties of atactic PNIPAM solutions with a concentration of 10 wt% by a particle tracking technique, in which the thermal motion of probe particles in the solution was tracked, in conjunction with Fourier-transform infrared spectroscopy, small-angle X-ray scattering measurements, fluorescence spectroscopy and confocal laser scanning microscopy. At temperatures far below T_{cp}, the solution exhibited one-phase homogeneous characteristics. After the PNIPAM aqueous solution was left undisturbed at a temperature just below T_{cp} (302 K), it formed a physical gel. Changing the size of probe particles for the tracking measurements, we found that the resultant gel was spatially heterogeneous in terms of its rheological properties at a length scale of approximately 50 to 100 nm. The gelation of the solution promoted by the formation of hydrophobic pearls in PNIPAM chains led to the formation of network junctions with the heterogeneity. The knowledge here obtained should be useful for understanding and controlling the phase behavior of the PNIPAM solution, thereby leading to the further development of thermoresponsive functional materials.

1. INTRODUCTION

Poly(*N*-isopropylacrylamide) (PNIPAM) is a representative thermoresponsive polymer exhibiting phase separation in water at elevated temperatures.[1–3] At room temperature, PNIPAM chains are homogenously dissolved in water with a random coil conformation. Upon heating, they collapse into a globular state due to the cooperative dehydration at a particular temperature, named the cloud point (T_{cp}).[4–6] Subsequently, globular chains aggregate with one another, resulting in phase separation, named the lower critical solution temperature (LCST).[7,8] Owing to its relatively sharp transition behavior at approximately 304 K, that is near to human body temperature, PNIPAM has been used as a building block in a wide range of products such as cell culture substrates,[9,10] drug carriers,[11,12] actuators,[13,14] sensors[15,16] and so forth.[17–19] To further promote the application of PNIPAM, its phase behavior should be better understood as a first benchmark.

The T_{cp} curve for the PNIPAM aqueous solution has often been regarded to be equivalent to the phase boundary curve, as for other polymer-solvent systems.[20–22] If that is the case, the phase diagram of the PNIPAM solution does not necessarily tally with our knowledge based on the Flory–Huggins theory.[3,23] For example, the T_{cp} value has been shown to be insensitive to the PNIPAM concentration[24] and decreases with decreasing molecular weight.[25,26] Besides, the chain end chemistry as well as the stereoregularity of PNIPAM chains has been reported to greatly affect the T_{cp} value.[27–29] Thus, to gain a better understanding of the phase behavior of the PNIPAM solution, great efforts have been devoted to both experimental[24–29] and theoretical[4,30] studies of the solution near the T_{cp}. For example, it has been reported that the viscosity of a PNIPAM aqueous solution with a relatively higher concentration dramatically increased with temperature near to the T_{cp}.[31] This result was explained in terms of the intermolecular chain association, which became more striking with the effective molecular weight of the PNIPAM chain. Another plausible explanation for the peculiar increase in

viscosity just below the T_{cp} is that PNIPAM chains associated with one another to form a physically-crosslinked network with a micrometer size, named microgel.[32,33] The formation of PNIPAM aggregates with a diameter of several tens of micrometers at a temperature below the T_{cp} has also been discussed.[21] Thus, it should be pointed out that although the origin of the peculiar viscosity behavior of the PNIPAM aqueous solution just below the T_{cp} should be a key to understanding the phase behavior, it remains unclear at the moment.

The structure of the PNIPAM solution at various length scales has been studied by well-established experimental techniques such as turbidimetry,[20,21,24–29] scattering experiments,[7,21,24,29,34] and infrared spectroscopy.[35,36] On the other hand, in the case of physical properties, characterization is generally limited to bulk methods.[24,28,31–33] Recently, new methods which can examine rheological properties at a local position have emerged.[37] A typical example of the local rheology, referred to as microrheology, is based on a particle tracking technique.[37–39] With this approach, probe particles are dispersed in a medium to be measured. Information on the local properties can be obtained by detecting the thermal motion of particles, since their movement reflects the rheological properties of their surrounding medium. This is a non-destructive approach to examining the local rheological properties, where the length scale of the detection can be altered by changing the particle size.[40–42] Moreover, investigating the behavior of individual particles can provide insight into the existence of any spatial heterogeneity, which is difficult to characterize using conventional bulk techniques.[43–46]

In this study, we first conducted a particle tracking measurement for an aqueous solution of PNIPAM at a temperature just below the T_{cp}. Once the PNIPAM solution was left undisturbed at the temperature for a while, it turned into a gel which remained transparent. To the best of our knowledge, the macroscopic gelation of the solution of ordinal, or atactic, PNIPAM at a temperature below the T_{cp} has not been reported, although such a gelation was

found for the aqueous solutions of isotactic-rich PNIPAM[47] and poly(*N*-isopropylmethacrylamide) (PNIPMAM).[48] The resultant gel was spatially heterogeneous in terms of its rheological properties at a length scale of approximately 50 to 100 nm.

2. EXPERIMENTAL

2.1. Materials. Atactic PNIPAM, which was purchased from Scientific Polymer Products, Inc., was purified by precipitation from an acetone solution with a large excess of *n*-hexane. The number-average molecular weight (M_n) and polydispersity index (M_w/M_n) of PNIPAM were determined by gel permeation chromatography using tetrahydrofuran containing 0.25 wt% tetrabutylammonium bromide as an eluent at 313 K.[49] The values of M_n and M_w/M_n referred to a poly(methyl methacrylate) standard were 193 k and 2.2, respectively.

Water used for a solution preparation was obtained by distillation with an Autostill WG33 (Yamato Scientific Co., Ltd.) and successive deionization with a Milli-Q Lab (Merck Millipore Co.). For particle tracking measurements, an aqueous dispersion of Fluoresbrite Yellow Green Microspheres, which are polystyrene (PS) particles containing a fluorescent dye, was purchased from Polysciences, Inc. The diameters (d_p) of the PS particles were 47 ± 3 nm, 116 ± 6 nm, 198 ± 9 nm and 513 ± 10 nm (hereafter denoted as 50 nm, 120 nm, 200 nm and 500 nm, respectively). Deuterated water (D_2O) and dimethyl sulfoxide (DMSO-d_6) were purchased from Wako Pure Chemical Industries, Ltd. Sodium 8-anilino-1-naphtalene-sulfonate (ANS) was purchased from Tokyo Chemical Industry Co., Ltd. and was used as received.

2.2. Transmittance measurements. The PNIPAM solution with a concentration of 10 wt % was sandwiched between two glass substrates with a 0.5 mm gap. The intensity of the light passing through the sample was monitored with a self-made apparatus equipped with a He-Ne laser with a wavelength of 633 nm. The temperature of the sample was controlled by a

thermostat system (SCR-SHQ-A, Sakaguchi E.H Voc Co.) having two silicone rubber heating plates (size: 45 × 45 mm), which were attached to the cover glasses. The actual temperature in the solution was monitored by a thermocouple thermometer (0.2×1P K-2-G-J2, Ninomiya Electric Wire Co., Ltd.).

2.3. Rheological measurements. Rheological measurements for the PNIPAM solution were performed by an MCR 310 rheometer (Anton Paar Japan K. K.). The solution was held between a sample stage and a cone-type plate with a diameter of 50 mm and a cone angle of 1°. For the frequency-sweep measurements, strain amplitude was set to 5 %, which was in a linear viscoelastic regime.

2.4. Particle tracking measurements. A portion of the PS particle dispersion was well-mixed into the aqueous PNIPAM solution. An aliquot of this dispersion was sandwiched between two cover glasses (Matsunami Glass Ind. Ltd.) with a 0.5 mm gap. The temperature of the sample was controlled by a modified setup previously reported (See the Supporting Information).[50,51] The actual temperature in the solution was monitored by a thermocouple thermometer (0.2×1P K-2-G-J2, Ninomiya Electric Wire Co., Ltd.). After heating to the desired temperatures of 294 and 302 K, the samples were left undisturbed for a period of 3 h prior to observation. We defined the aging time of zero as a moment when the sample temperature reached a target value.

Our approach used for particle tracking was based on an inverted microscope, a Nikon ECLIPSE Ti, with an NA 1.30 oil-immersion objective lens (Plan Fluor 100×, Nikon), as reported elsewhere.[41] A mercury lamp shone through an excitation filter (passband: 426 – 446 nm) housed in a filter block (CFP, Nikon Instech Co., Ltd.) illuminated the sample. The florescence images were acquired by an electron multiplying charge coupled device (EM-CCD)

camera (Ixon Ultra 897, Andor Technology Co., Ltd.) at a frame rate of 24 Hz. The imaging software NIS-Elements AR-3.22 (Nikon Instech Co., Ltd.) was used for trajectory analysis of the particles. A total of 20 particles were individually tracked in each sample. Each particle was monitored 10 times to average the diffusion behaviors.

2.5. Fourier-transform infrared spectroscopy. The PNIPAM solutions were prepared using D_2O. Each sample was sandwiched between CaF_2 windows with a 15 μm gap. The FT-IR spectra were recorded using an FT/IR-620 spectrometer (JASCO Co.) with a triglycine sulfate detector. All spectra were obtained at a resolution of 4 cm^{-1} and 64 scans.

2.6. Small-angle X-ray scattering measurements. Small-angle X-ray scattering (SAXS) experiments were performed at the BL03XU beamline in SPring-8 (Japan).[52] The wavelength of the incident X-rays and the sample-to-detector distance were 0.10 nm and 2,314 mm, respectively. The PNIPAM solution filled in a quartz capillary was installed in a temperature-controlled stage. The scattered X-ray intensities were recorded using a PILATUS 1M (DECTRIS Ltd.). By circular averaging a two-dimensional pattern on the detector, we obtained a one-dimensional scattering profile of the sample.

2.7. Fluorescence spectroscopy and confocal laser scanning microscopy. The PNIPAM solution containing 60 μM of ANS was placed in a quartz cell having a path length of 10 mm. The fluorescence spectra were recorded using an F-4500 Spectrophotometer (Hitachi High-Technologies Co.). The measurements were made at 294 and 302 K, which were maintained by using a temperature-controlled water circulator, NCB-1200 (Tokyo Rikakikai Co., Ltd.).

For the confocal laser scanning microscopic (CLSM) observation, the PNIPAM solution containing ANS was sandwiched between two cover glasses with a 0.5 mm gap. The

temperature of the sample was controlled by the same setup as the particle tracking measurements. CLSM images were acquired by a Nikon C2+ Confocal Microscope System with a DAPI filter block (Nikon Instech Co., Ltd.). The pinhole size used corresponded to the depth of the focal plane of 40 μm.

3. RESULTS AND DISCUSSION

3.1. Physical gelation. A transparent aqueous solution of PNIPAM was obtained by dissolving the PNIPAM powder into pure water at 283 K to ensure the one-phase solution status prior to further experiments. The concentration of PNIPAM was kept at 10 wt%, which was much higher than the overlap concentration of 1.2 wt%. Upon heating at a rate (ν) of 0.1 K·min^{-1}, Figure 1(a) shows the change in light transmittance for the PNIPAM aqueous solution. Once the solution temperature went beyond 304 K, the transmittance started to decrease. The temperature at which the transmittance started to decrease was determined and denoted as T_{cp}'. The corresponding T_{cp}' at different ν in a wide range of 0.017 – 0.2 K·min^{-1} was obtained and plotted against the heating rate as shown in Figure 1(b). It is clear that the T_{cp}' slightly decreased as the heating rate was reduced. By the linear extrapolation of T_{cp}' to the zero heating rate, the T_{cp} value of the PNIPAM solution was rigorously determined to be 304.4 K.

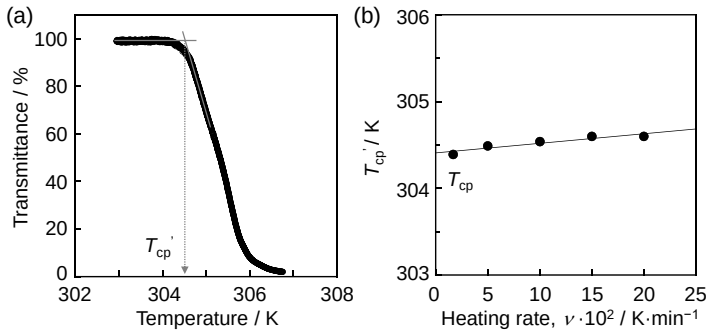

Figure 1 Change in light transmittance for the PNIPAM-water mixture during the heating process with a rate (ν) of 0.1 K·min^{-1}, and (b) ν dependence of T_{cp}', at which the transmittance started to decrease upon heating.

Figure 2 shows photographic images of the time-variation in the physical state of the PNIPAM-water mixtures before and after aging at (a) 294 and (b) 302 K, respectively. After being aged for 3 h at 294 K, the initial mixture still remained in a transparent fluid state. A fluid state was also seen at time $t = 0$ when the solution was rapidly brought to a controlled temperature of 302 K, which was just below the T_{cp}. After the mixture was left undisturbed at 302 K for a few hours however, it turned into a macroscopic gel state without any loss of transparency. Such a transparent PNIPAM gel was unexpected and remarkable because atactic PNIPAM was used in our solution, as discussed in the latter section. To validate the formation of the physical gel at 302 K, the aged solutions were further quantitatively examined by rheological measurements.

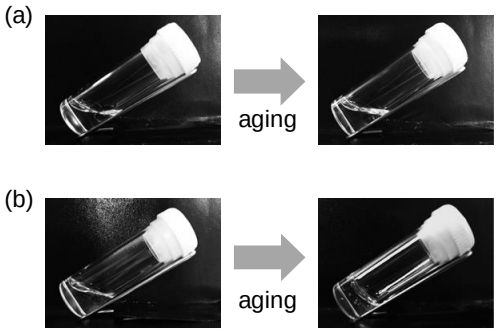

Figure 2 Photographic images showing the change in the fluidity of the PNIPAM-water mixtures during the aging process for 3 h at (a) 294 and (b) 302 K.

Figure 3 shows the frequency (ω) dependence of storage (G') and loss moduli (G'') for the PNIPAM-water mixtures after being aged for 3 h, which was long enough to reach dynamic equilibrium, at (a) 294 and (b) 302 K. For the solution aged at 294 K, G'' was larger than G' at a given frequency and both G' and G'' simply increased with increasing ω. Notably, in a low ω region, G' and G'' were found to follow the scaling law of $\omega^{1.9}$ and $\omega^{1.0}$, respectively. This is commonly seen for a homogeneous viscous liquid.[33] For the solution aged at 302 K on the other hand, G' was larger than G'' across the entire ω range used (10^{-2} – 10^{2} rad·s^{-1}). More importantly, an evident plateau of G' was identified and this was an indication that the

system was in a gel state.[42,53]

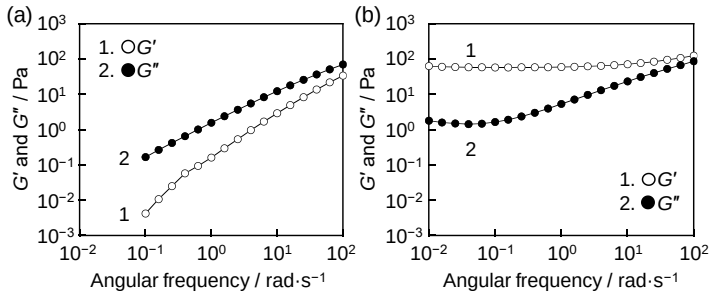

Figure 3 Frequency (ω) dependence of storage (G') and loss moduli (G'') for the PNIPAM-water mixtures aged for 3 h at (a) 294 and (b) 302 K.

To examine how the aging temperature affects the gelation, G' and G'' for the PNIPAM-water mixtures that were aged for 3 h at various temperatures were examined. Figure 4 shows G' and G'' for the aged PNIPAM aqueous solution at ω of 1 rad·s^{-1} as a function of aging temperature. Both G' and G'' increased with increasing temperature. However, the increment of G' with temperature was larger than that of G''. Consequently, the magnitude relationship between G' and G'' was reversed at a temperature in the range of 300 to 302 K. Thus, it is most likely that the PNIPAM-water mixture changed to a gel state after aging at a temperature just below the T_{cp} of 304.4 K. Here, it is noteworthy that as the temperature increased from 294 to 302 K, the complex viscosity increased from 0.11 to 60 Pa·s. Thus, it is plausible that the gelation here observed is related to the dramatic increase in the viscosity of the PNIPAM solution at a temperature near to the T_{cp}, which was previously reported.[31]

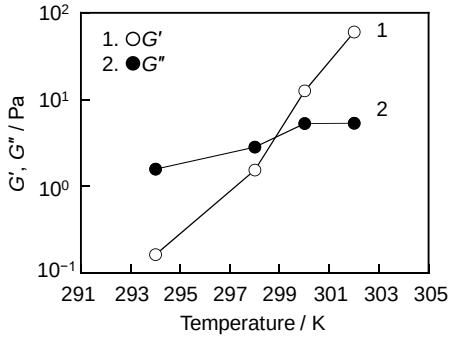

Figure 4 G' and G'' for the PNIPAM-water mixture aged for 3 h at a frequency (ω) of 1 rad·s^{-1} as a function of aging temperature.

3.2. Spatial heterogeneity. The mixtures obtained after aging for 3 h at 294 and 302 K were subjected to particle tracking measurements. To examine different length scales, PS particles with various d_ps ranging from 50 to 500 nm were used. On the basis of the two-dimensional trajectories of individual particles, the mean-square-displacement, $\langle \Delta r^2(t) \rangle$, was obtained from the following equation;[37,39,41]

$$\left\langle \Delta r^2(t) \right\rangle = \frac{1}{N} \sum_{i=1}^{N} \left\{ \boldsymbol{r}_i(t) - \boldsymbol{r}_i(0) \right\}^2 \tag{1}$$

where $r_i(0)$ and $r_i(t)$ are the positions of a particle i at the lag time of 0 and t, and N is the number of data sets analyzed. The $\langle \Delta r^2(t) \rangle$ value quantitatively reflects the averaged travel distance of a particle from the original position after a time of t. From the slope (n) of the double logarithmic plot of $\langle \Delta r^2(t) \rangle$ against t, the type of particle motion can be discussed.[37,54,55]

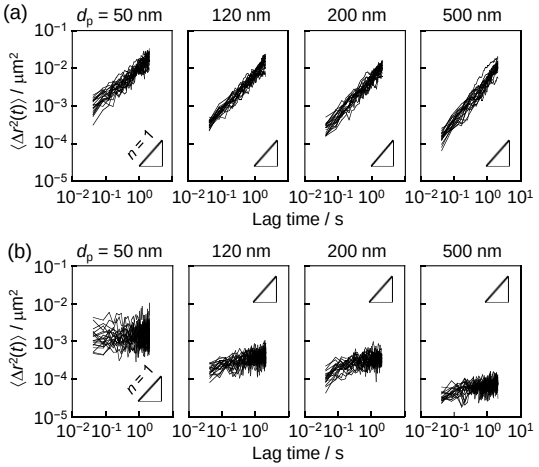

Figure 5 Double logarithmic plots of $\langle \Delta r^2(t) \rangle$ against t for PS particles having d_ps of 50 nm, 120 nm, 200 nm and 500 nm in the PNIPAM-water mixtures aged for 3 h at (a) 294 and (b) 302 K.

Figure 5 shows double logarithmic plots of $\langle \Delta r^2(t) \rangle$ against t for PS particles embedded in the PNIPAM-water mixtures aged for 3 h at (a) 294 and (b) 302 K. Each solid line was obtained by taking an average of 10 data sets for a single particle. The slope of the hypotenuse of right-angled triangles in the figure corresponds to 1. For the mixture aged at 294 K, the n value for all plots using particles with d_ps of 50 – 500 nm was regarded as 1. This means that

the motion of particles was based on the random walk statistical model, as is commonly seen for particle diffusion in a homogeneous fluid.[37,54] However, this was not the case for the mixture aged at 302 K. For 500 nm-particles, the *n* values for all plots were less than 1. As the particle size decreased, the $\langle \Delta r^2(t) \rangle$ value slightly increased but the *n* of the plots remained smaller than 1. That is, although the $\langle \Delta r^2(t) \rangle$ value was larger for 50 nm-particles than for 500 nm-ones, the *n* of 1 could be barely discerned even for 50 nm-particles. This implies that 50 nm-particles did not travel any great distance but merely fluctuated in amplitude,[55] which may correspond to the size of a less-dense region, as discussed later.

To address the $\langle \Delta r^2(t) \rangle$ variation, the shape of the probability distribution of $\langle \Delta r^2(t) \rangle$ normalized by the ensemble average $\langle \Delta r^2(t) \rangle_{ave}$ was evaluated (See the Supporting Information). When the shape can be expressed by a simple Gaussian function, or a symmetric shape, with a central value of 1, it can be claimed that the system is homogeneous in terms of its rheological properties.[41,56] By contrast, if the distribution of the normalized $\langle \Delta r^2(t) \rangle$ is far from the Gaussian, the system should be heterogeneous.[41,43]

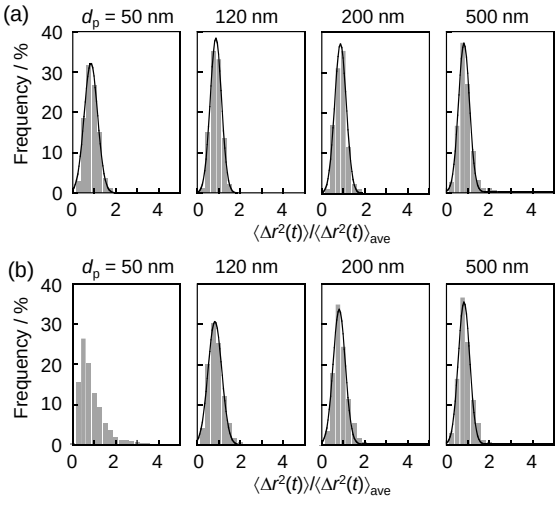

Figure 6 Probability distributions of the normalized $\langle \Delta r^2(t) \rangle$ values for PS particles with d_ps of 50 to 500 nm in the PNIPAM-water mixtures aged for 3 h at (a) 294 and (b) 302 K.

Figure 6 shows the distributions of the normalized $\langle \Delta r^2(t) \rangle$ for particles with d_ps of 50 – 500 nm in the PNIPAM-water mixtures aged for 3 h at (a) 294 and (b) 302 K. For the mixture

aged at 294 K, the profiles of particles with d_ps of 50 – 500 nm all provided a Gaussian distribution, indicating that the system was homogenous at all length scales probed. For the mixture aged at 302 K, while the distribution for the particles with d_ps of 120 nm – 500 nm were Gaussian in shape, a non-Gaussian distribution was observed for 50 nm-particles. Thus, it is apparent that the PNIPAM-water mixture aged at a temperature just below the T_{cp} was spatially heterogeneous at the length scale of 50 – 120 nm in terms of its rheological properties.

To study the evolution of the heterogeneity, the thermal motion of particles was examined during the aging process at 302 K. Figure 7 shows (a) plots of $\langle \Delta r^2(t) \rangle$ against t and (b) the distributions of the normalized $\langle \Delta r^2(t) \rangle$ for 50 nm-particles in the PNIPAM-water mixture at various stages of the aging process. At 0 and 1 h aging, n of all plots was equal to 1. With increasing aging time, however, n of the plots decreased and eventually became less than 1. These findings indicate that particles were increasingly trapped during the aging process.[46,54] In addition, it is noteworthy that the distribution changed from Gaussian to non-Gaussian with increasing aging time. That is, the aging process, which induced the macroscopic gelation, was accompanied by the evolution of the heterogeneous environment.

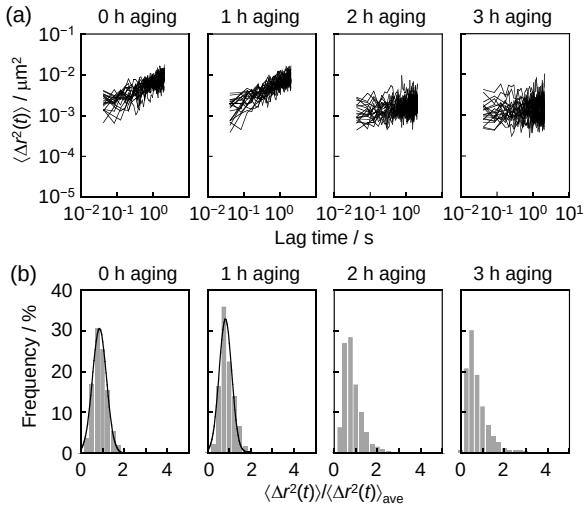

Figure 7 (a) Plots of $\langle \Delta r^2(t) \rangle$ against t and (b) distributions of the normalized $\langle \Delta r^2(t) \rangle$ value for 50 nm-PS particles in the PNIPAM-water mixture during the aging process at 302 K.

3.3. Aggregation states. It is well known that the phase separation behavior strongly depends

on the stereoregularity of PNIPAM.[7,27,28,29] For example, the T_{cp} for the PNIPAM solution decreases with increasing *meso* diad content (f_m) of PNIPAM.[7,27] It has recently been reported that while macroscopic gelation occurred for the solution of isotactic-rich PNIPAM having f_m of 64 % upon heating at a temperature below T_{cp}, no gelation occurred for atactic PNIPAM.[47] The gelation was explained in terms of the network formation via the intermolecular association, which took place faster than the formation of globules and aggregates of isotactic-rich PNIPAM.[7] In fact, molecular dynamics simulations have revealed that the intermolecular interaction between isotactic-rich PNIPAM chains is stronger than that between atactic-rich ones.[57,58] To confirm whether the above hypothesis can be extended to the current study, the tacticity of PNIPAM used here was examined with ^{1}H-NMR spectroscopy (See Figure S1 in the Supporting Information). Based on the integral ratio of the splitting methylene proton signals of the main chain, the f_m value was determined to be 48 %. That is, the PNIPAM used was atactic. Thus, the gelation and thereby the heterogeneity evolution detected by particle tracking may not be simply understood on the basis of the hypothesis proposed for isotactic-rich PNIPAM.

The PNIPAM-water mixture was then structurally characterized. Using FT-IR spectroscopy, as shown in Figure S2, the dehydration and the concurrent formation of hydrogen bonds among PNIPAM chains was not discerned even after aging for 3 h at 302 K. SAXS measurement revealed that the scattering intensity, or the fluctuation of the electron density in the solution, increased upon aging at 302 K, as shown in Figure S3. The fitting analysis of the scattering profile using a combinational function of the Ornstein-Zernike and Guinier functions revealed the existence of a cluster, composed of the intermolecular association of segments, with a radius of gyration R_g of 7.5 nm. However, such a cluster may not be directly associated with what was observed by the particle tracking measurement because the length scale of the structure accessible by the two methods was not the same. Deferring a proposal of the

aggregation structure of atactic PNIPAM in the aqueous solution at 302 K to the final section, CLSM was used with sodium 8-anilino-1-naphthalenesulfonate (ANS) as a fluorescent probe.

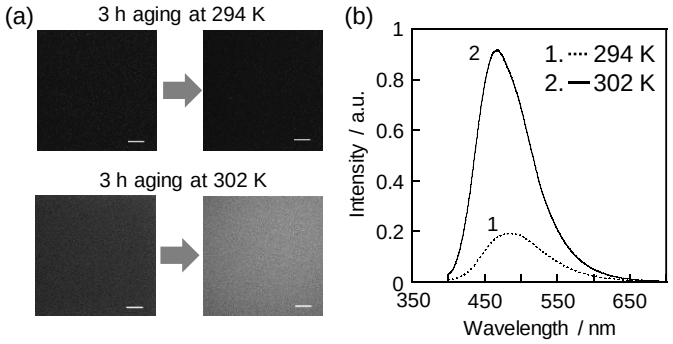

Figure 8 (a) CLSM images for the PNIPAM-water mixtures containing ANS during the aging process at 294 and 302 K, and (b) corresponding fluorescence spectra of ANS in the PNIPAM-water mixture aged at these temperatures. White bars in panel (a) correspond to a length of 10 μm.

The ANS dye emits stronger fluorescence in a hydrophobic environment than in a hydrophilic one, making it possible to stain a hydrophobic region in a system if any exists.[59] Figure 8(a) shows CLSM images for the PNIPAM-water mixtures containing ANS during the aging process at 294 and 302 K. The mixture aged at 294 K provided a dark image regardless of the aging time, indicating that the surrounding medium for ANS was relatively hydrophilic even after the aging. The dark image was also observed for the mixture at 302 K before aging. After 3 h however, the image became brighter. Fluorescence spectra also confirmed this behavior, as shown in Figure 8(b). The emission from ANS in the mixture aged for 3 h at 302 K was much stronger than that similarly aged at 294 K. These results make it clear that relatively hydrophobic regions were formed upon aging at 302 K. Taking into account that the main chain part and the isopropyl side chain portion of PNIPAM are hydrophobic, it seems reasonable to consider that the hydrophobic region should be composed of PNIPAM-rich domains. Here, it should be noted that the CLSM image obtained for the mixture aged for 3 h at 302 K was featureless. This was simply because the size of PNIPAM-rich domains was smaller than the limit of the spatial resolution of our CLSM, ca. 200 nm.

We finally combined the results obtained in the above to provide a plausible morphological model. Figure 9 shows a schematic illustration of the hierarchical aggregation state of the PNIPAM-water mixture aged at 302 K including particles for the tracking measurement. A bulk rheometer revealed that the gelation of the PNIPAM solution occurred at 302 K. The physical gelation could be macroscopically seen once a vial including the gel was tilted. Particle tracking measurements with various d_ps revealed the existence of the heterogeneity with a length scale of approximately 50 to 100 nm, which was possibly composed of dense and less-dense regions of PNIPAM chains. This is consistent with the featureless image obtained by CLSM observation, which also verified the existence of hydrophobic and hydrophilic regions at this temperature. Besides, our SAXS results showed the existence of aggregates with R_g of approximately 7.5 nm in the physical gel. The aggregates, or clusters, were likely formed via "hydrophobic pearls", which were defined as a compact spherical globule composed of dehydrated segments,[4] and thus, the R_g should be regarded as the radius of junction domains for the developed physical gel. Thus, it is apparent that the clusters in the dense regions at a nanometer scale are what were observed by SAXS analysis. One point that should be finally discussed is whether the spatial heterogeneity, or the concentration fluctuation, was formed first followed by gelation, or vice-versa. FT-IR spectroscopy did not show any clear evidence that the dehydration of PNIPAM chains proceeded at 302 K. Thus, it seems unlikely that the concentration fluctuation occurred first followed by gelation. This means that the dehydration of PNIPAM chains slowly occurred during the aging process, resulting in the physical gelation via "hydrophobic pearls". This then led to the eventual formation of hydrophobic domains, and thereby hydrophilic ones. This scenario is consistent with a recent publication dealing with the physical hydrogel of PNIPMAM.[48]

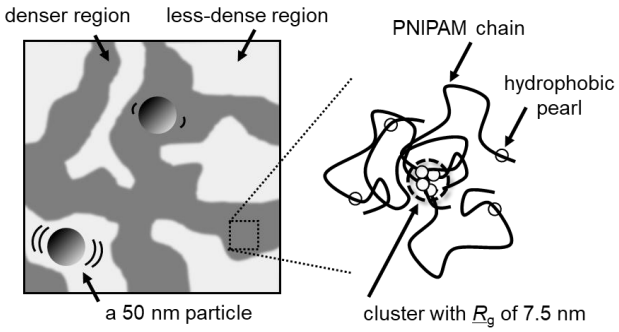

Figure 9 Schematic illustration of the aggregation structure of the PNIPAM-water mixture aged at 302 K.

4. CONCLUSIONS

We first found that once the aqueous solution of atactic PNIPAM with a concentration of 10 wt% was left undisturbed at a temperature just below the T_{cp} (ca. 2 K lower), it turned into a transparent gel. Particle tracking experiments clearly revealed that the gel so obtained was spatially heterogeneous in terms of its rheological properties, as evidenced by the variation in the particle motion depending on the location at which a particle existed. With varying of the particle size, it was found that the characteristic length scale of the heterogeneity was 50 to 100 nm. The heterogeneity evolved during the gelation process. FTIR spectroscopy confirmed that, upon the gelation process, the dehydration of PNIPAM chains and the concurrent formation of hydrogen bonds among chains did not occur. SAXS measurement suggested the existence of the cluster formed by the intermolecular association. The clustering of PNIPAM chains led to the development of the PNIPAM-rich domains and water-rich regions, as evidenced by the CLSM observation. The dehydration of PNIPAM chains slowly occurred during the aging process, resulting in the physical gelation via “hydrophobic pearls”. This eventually led to the heterogeneous structure. Finally, it is also remarked that the heterogeneous structure based on the gelation could be a reason for the increase in viscosity of the PNIPAM solution at a temperature near to the T_{cp}, which was previously reported.[31] The knowledge here obtained should be useful for understanding and controlling the phase behavior

of the PNIPAM solution, thereby leading to the further development of functional materials using PNIPAM as a building block.

ACKNOWLEDGMENTS

This research was partly supported by JSPS KAKENHI for Scientific Research (B) (no. JP20H02790) (K.T.), (no. JP19H02780) (A.S.). We are also grateful for support from the JST-Mirai Program (JPMJMI18A2) (K.T.). The synchrotron radiation facilities experiments were performed at BL03XU (Frontier Soft Matter Beamline, FSBL) in the SPring-8 with the approval of the Japan Synchrotron Radiation Research Institute (JASRI). (Proposal: 2018A7222, 2018B7272). We thank Mr. Junichiro Koike of DIC Corporation for his help with the SAXS measurements.

SUPPORTING INFORMATION

Supporting Information is available free of charge on the ACS Publications website.

Experimental detail and characterization data by proton nuclear magnetic resonance spectroscopy, particle tracking measurement, Fourier-transform infrared spectroscopy and small-angle X-ray scattering measurement.

REFERENCES

(1) Heskins, M.; Guillet, J. E. Solution Properties of Poly(*N*-isopropylacrylamide). *J. Macromol. Sci., Chem.* **1968**, *2*, 1441−1455.

(2) Schild, H. G. Poly(*N*-isopropylacrylamide): Experiment, Theory and Application. *Prog. Polym. Sci.* **1992**, *17*, 163−249.

(3) Halperin, A.; Kröger, M.; Winnik, F. M. Poly(*N*-isopropylacrylamide) Phase Diagrams: Fifty Years of Research. *Angew. Chem. Int. Ed.* **2015**, *54*, 15342−15367.

(4) Okada, Y.; Tanaka, F. Cooperative Hydration, Chain Collapse, and Flat LCST Behavior in

Aqueous Poly(*N*-isopropylacrylamide) Solutions. *Macromolecules* **2005**, *38*, 4465−4471.

(5) Shiraga, K.; Naito, H.; Suzuki, T.; Kondo, N.; Ogawa, Y. Hydration and Hydrogen Bond Network of Water during the Coil-to-Globule Transition in Poly(*N*-isopropylacrylamide) Aqueous Solution at Cloud Point Temperature. *J. Phys. Chem. B* **2015**, *119*, 5576−5587.

(6) Tavagnacco, L.; Zaccarelli, E.; Chiessi, E. On the Molecular Origin of the Cooperative Coil-to-globule Transition of Poly(*N*-isopropylacrylamide) in Water. *Phys. Chem. Chem. Phys.* **2018**, *20*, 9997−10010.

(7) Nishi, K.; Hiroi, T.; Hashimoto, K.; Fujii, K.; Han, Y.-S.; Kim, T.-H.; Katsumoto, Y.; Shibayama, M. SANS and DLS Study of Tacticity Effects on Hydrophobicity and Phase Separation of Poly(*N*-isopropylacrylamide). *Macromolecules* **2013**, *46*, 6225−6232.

(8) Balu, C.; Delsanti, M.; Guenoun, P. Colloidal Phase Separation of Concentrated PNIPAm Solutions. *Langmuir* **2007**, *23*, 2404−2407.

(9) Okano, T.; Yamada, N.; Sakai, H.; Sakurai, Y. A Novel Recovery System for Cultured Cells using Plasrna-Treated Polystyrene Dishes Grafted with Poly(*N*-isopropylacrylarnide). *J. Biomed. Mater. Res.* **1993**, *27*, 1243−1251.

(10) Ohashi, K.; Yokoyama, T.; Yamato, M.; Kuge, H.; Kanehiro, H.; Tsutsumi, M.; Amanuma, T.; Iwata, H.; Yang, J.; Okano, T.; Nakajima, Y. Engineering Functional Two- and Three-Dimensional Liver Systems in vivo Using Hepatic Tissue Sheets. *Nature Medicine* **2007**, *13*, 880−885.

(11) Liu, M.; Song, X.; Wen, Y. T.; Zhu, J. L.; Li, J. Injectable Thermoresponsive Hydrogel Formed by Alginate-*g*-Poly(*N*-isopropylacrylamide) That Releases Doxorubicin-Encapsulated Micelles as a Smart Drug Delivery System. *ACS Appl. Mater. Interfaces* **2017**, *9*, 35673−35682.

(12) Ida, S; Toyama, Y; Takeshima, S; Kanaoka, S. Thermoresponsive Core Cross-Linked Star-Shaped Poly(*N*-isopropylacrylamide) for Reversible and Controlled Aggregation of Nanoscale Molecular Units. *Polym. J.* **2020**, *52*, 359−363.

(13) Suzuki, A.; Ishii, T.; Maruyama, Y. Optical Switching in Polymer Gels. *J. Appl. Phys.* **1996**, *80*, 131−136.

(14) Yao, C.; Liu, Z.; Yang, C.; Wang, W.; Ju, X.-J.; Xie, R.; Chu, L.-Y. Poly(*N*-

isopropylacrylamide)-Clay Nanocomposite Hydrogels with Responsive Bending Property as Temperature-Controlled Manipulators. *Adv. Funct. Mater*. **2015**, *25*, 2980–2991.

(15) Holtz, J. H. Asher, S. A. Polymerized Colloidal Crystal Hydrogel Films as Intelligent Chemical Sensing Materials. *Nature* **1997**, *389*, 829–832.

(16) Hoare, T.; Pelton, R. Engineering Glucose Swelling Responses in Poly(*N*-isopropylacrylamide)-Based Microgels. *Macromolecules* **2007**, *40*, 670–678.

(17) Zhao, X. Q.; Zhang, J.; Zhao, Y. L. Synthesis and Properties of Penta-Responsive ABC Star Quaterpolymers. *Polym. J*. **2020**, *52*, 153−163.

(18) Kotsuchibashi, Y. Recent Advances in Multi-Temperature-Responsive Polymeric Materials. *Polym. J*. **2020**, *52*, 681−689.

(19) Minato, H.; Nishizawa, Y.; Uchihashi, T.; Suzuki, D. Thermoresponsive Structural Changes of Single Poly(*N*-isopropyl acrylamide) Hydrogel Microspheres under Densely Packed Conditions on a Solid Substrate. *Polym. J*. **2020**, *52*, 1137−1141.

(20) Kawaguchi, T.; Kojima, Y.; Osa, M.; Yoshizaki, T. Cloud Points in Aqueous Poly(*N*-isopropylacrylamide) Solutions. *Polym. J*. **2008**, *40*, 455−459.

(21) Kawaguchi, T.; Kobayashi, K.; Osa, M.; Yoshizaki, T. Is a "Cloud-Point Curve" in Aqueous Poly(*N*-isopropylacrylamide) Solution Binodal? *J. Phys. Chem. B* **2009**, *113*, 5440–5447.

(22) Shimomoto, H.; Yamada, T.; Itoh, T.; Ihara, E. Carbon-Carbon Main Chain Polymer with Accumulated Oligo(ethylene glycol)-Substituted Cyclotriphosphazenes: Study on the LCST-Type Phase Separation of Organic-Inorganic Poly(substituted methylene)s. *Polym. J*. **2020**, *52*, 51−56.

(23) Matsuda, Y.; Miyazaki, Y.; Sugihara, S.; Aoshima, S.; Saito, K.; Sato, T. Phase Separation Behavior of Aqueous Solutions of a Thermoresponsive Polymer. *J. Polym. Sci. B Polym. Phys.* **2005**, *43*, 2937–2949.

(24) Kobayashi, K.; Yamada, S.; Nagaoka, K.; Kawaguchi, T.; Osa, M.; Yoshizaki, T. Characterization of Linear Poly(*N*-isopropylacrylamide) and Cloud Points in its Aqueous Solutions. *Polym. J*. **2009**, *41*, 416−424.

(25) Tong, Z.; Zeng, F.; Zheng, X. Inverse Molecular Weight Dependence of Cloud Points for

Aqueous Poly(*N*-isopropylacrylamide) Solutions. *Macromolecules* **1999**, *32*, 4488−4490.

(26) Tsuboi, Y.; Tada, T.; Shoji, T.; Kitamura, N. Phase-Separation Dynamics of Aqueous Poly(*N*-isopropylacrylamide) Solutions: Characteristic Behavior of the Molecular Weight and Concentration Dependences. *Macromol. Chem. Phys.* **2012**, *213*, 1879–1884.

(27) Ray, B.; Okamoto, Y.; Kamigaito, M.; Sawamoto, M.; Seno, K.; Kanaoka, S.; Aoshima, S. Effect of Tacticity of Poly(*N*-isopropylacrylamide) on the Phase Separation Temperature of Its Aqueous Solutions. *Polym. J.* **2005**, *37*, 234−237.

(28) Biswas, C. S.; Mitra, K.; Singh, S.; Ramesh, K.; Misra, N.; Maiti, B.; Panda, A. K.; Maiti, P.; Kamigaito, M.; Okamoto, Y.; Ray, B. Study of the Effect of Isotacticity on Some Physical Properties of Poly(*N*-isopropylacrylamide). *Colloid Polym. Sci.* **2015**, *293*, 1749–1757.

(29) Tada, T.; Hirano, T.; Ute, K.; Katsumoto, Y.; Asoh, T.-A.; Shoji, T.; Kitamura, N.; Tsuboi, Y. Effects of Syndiotacticity on the Dynamic and Static Phase Separation Properties of Poly(*N*-isopropylacrylamide) in Aqueous Solution. *J. Phys. Chem. B* **2016**, *120*, 7724−7730.

(30) Tanaka, F.; Katsumoto, Y.; Nakano, S.; Kita, R. LSCT Phase Searation and Thermoreversble Gelation in Aqueous Solutions of Stereo-Controlled Poly(*N*-isopropylacrylamide)s. *React. Funct. Polym.* **2013**, *73*, 894–897.

(31) Tam, K. C.; Wu, X. Y.; Pelton, R. H. Viscometry – a Useful Tool for Studying Conformational Changes of Poly(*N*-isopropylacrylamide) in Solutions. *Polymer* **1992**, *33*, 436−438

(32) Zheng, X.; Tong, Z.; Xie, X.; Zeng, F. Phase Separation in Poly(*N*-isopropylacrylamide)/Water Solutions I. Cloud Point Curves and Microgelation. *Polym. J.* **1998**, *30*, 284−288.

(33) Zeng, F.; Zheng, X.; Tong, Z. Network Formation in Poly(*N*-isopropyl acrylamide)/Water Solutions during Phase Separation. *Polymer* **1998**, 39, 1249−1251.

(34) Meier-Koll, A.; Pipich, V.; Busch, P.; Papadakis, C. M.; Müller-Buschbaum, P. Phase Separation in Semidilute Aqueous Poly(*N*-isopropylacrylamide) Solutions. *Langmuir* **2012**, *28*, 8791−8798.

(35) Maeda, Y.; Higuchi, T.; Ikeda, I. Change in Hydration State during the Coil−Globule Transition of Aqueous Solutions of Poly(*N*-isopropylacrylamide) as Evidenced by FTIR Spectroscopy. *Langmuir* **2000**, *16*, 7503−7509.

(36) Sun, B.; Lin, Y.; Wu, P.; Siesler, H. W. A FTIR and 2D-IR Spectroscopic Study on the

Microdynamics Phase Separation Mechanism of the Poly(*N*-isopropylacrylamide) Aqueous Solution. *Macromolecules* **2008**, *41*, 1512−1520.

(37) Waigh, T. A. Microrheology of Complex Fluids. *Rep. Prog. Phys.* **2005**, *68*, 685−742.

(38) Valentine, M. T.; Kaplan, P. D.; Thota, D.; Crocker, J. C.; Gisler, T.; Prud'homme, R. K.; Beck, M.; Weitz, D. A. Investigating the Microenvironments of Inhomogeneous Soft Materials with Multiple Particle Tracking. *Phys. Rev. E* **2001**, *64*, 061506.

(39) Penaloza, D. P.; Hori, K.; Shundo, A.; Tanaka, K.; Spatial Heterogeneity in a Lyotropic Liquid Crystal with Hexagonal Phase. *Phys. Chem. Chem. Phys.* **2012**, *14*, 5247−5250.

(40) Yamamoto, N.; Ichikawa, M.; Kimura, Y. Local Mechanical Properties of a Hyperswollen Lyotropic Lamellar Phase. *Phys. Rev. E* **2010**, *82*, 021506.

(41) Shundo, A.; Hori, K.; Penaloza, D. P.; Matsumoto, Y.; Okumura, Y.; Kikuchi, H.; Lee, K. E.; Kim, S. O.; Tanaka, K. Hierarchical Spatial Heterogeneity in Liquid Crystals Composed of Graphene Oxides. *Phys. Chem. Chem. Phys.* **2016**, *18*, 22399−22406.

(42) Matsumoto, Y.; Shundo, A.; Ohno, M.; Tsuruzoe, N.; Goto, M.; Tanaka, K. Mesoscopic Heterogeneity in Pore Size of Supramolecular Networks. *Langmuir* **2018**, *34*, 7503−7508.

(43) Tseng, Y.; Wirtz, D. Mechanics and Multiple-Particle Tracking Microheterogeneity of α-Actinin-Cross-Linked Actin Filament Networks. *Biophys. J.* **2001**, 81, 1643−1656.

(44) Penaloza, D. P.; Shundo, A.; Matsumoto, K.; Ohno, M.; Miyaji, K.; Goto, M.; Tanaka, K. Spatial Heterogeneity in the Sol–Gel Transition of a Supramolecular System. *Soft Matter* **2013**, *9*, 5166−5172.

(45) Matsumoto, Y.; Shundo, A.; Ohno, M.; Tsuruzoe, N.; Goto, M.; Tanaka, K. Evolution of Heterogeneity Accompanying Sol–Gel Transitions in a Supramolecular Hydrogel. *Soft Matter* **2017**, *13*, 7433−7440.

(46) Aoki, M.; Shundo, A.; Kawahara, R.; Yamamoto, S.; Tanaka, K. Mesoscopic Heterogeneity in the Curing Process of an Epoxy−Amine System. *Macromolecules* **2019**, *52*, 2075−2082.

(47) Nakano, S.; Ogiso, T.; Kita, R.; Shinyashiki, N.; Yagihara, S.; Yoneyama, M.; Katsumoto, Y. Thermoreversible Gelation of Isotactic-Rich Poly(*N*-isopropylacrylamide) in Water. *J. Chem.*

Phys. **2011**, *135*, 114903.

(48) Ko, C.-H.; Claude, K.-L.; Niebuur, B.-J.; Jung, F. A.; Kang, J.-J.; Schanzenbach, D.; Frielinghaus, H.; Barnsley, L. C.; Wu, B.; Pipich, V.; Schulte, A.; Müller-Buschbaum, P.; Laschewsky, A.; Papadakis, C. M. Temperature-Dependent Phase Behavior of the Thermoresponsive Polymer Poly(*N*-isopropylmethacrylamide) in an Aqueous Solution. *Macromolecules* **2020**, *53*, 6816−6827.

(49) Schilli, C.; Lanzendörfer, M. G.; Müller, A. H. E. Benzyl and Cumyl Dithiocarbamates as Chain Transfer Agents in the RAFT Polymerization of *N*-Isopropylacrylamide. In Situ FT-NIR and MALDI-TOF MS Investigation. *Macromolecules* **2002**, *35*, 6819−6827.

(50) Shundo, A.; Hori, K.; Penaloza, D. P.; Tanaka, K. Optical Tweezers with Fluorescence Detection for Temperature-Dependent Microrheological Measurements. *Rev*. *Sci*. *Instrum*. **2013**, *84*, 014103.

(51) Wu, Y.; Shundo, A.; Yasukochi, Y.; Tanaka, K. Time-Dependent Heterogeneity in Polyacrylic Pressure Sensitive Adhesive. *Eur. Polym. J*. **2020**, *134*, 109812-1−5.

(52) Masunaga, H.; Ogawa, H.; Takano, T.; Sasaki, S.; Goto, S.; Tanaka, T.; Seike, T.; Takahashi, S.; Takeshita, K.; Nariyama, N.; Ohashi, H.; Ohata, T.; Furukawa, Y.; Matsushita, T.; Ishizawa, Y.; Yagi, N.; Takata, M.; Kitamura, H.; Sakurai, K.; Tashiro, K.; Takahara, A.; Amamiya, Y.; Horie, K.; Takenaka, M.; Kanaya, T.; Jinnai, H.; Okuda, H.; Akiba, I.; Takahashi, I.; Yamamoto, K.; Hikosaka, M.; Sakurai, S.; Shinohara, Y.; Okada, A.; Sugihara, Y. Multipurpose Softmaterial SAXS/WAXS/GISAXS Beamline at SPring-8. *Polym*. *J*. **2011**, *43*, 471−477.

(53) Kavanagh, G. M.; Ross-Murphy, S. B. Rheological Characterisation of Polymer Gels. *Prog*. *Polym*. *Sci*. **1998**, *23*, 533.

(54) Oppong, F. K.; Coussot, P.; de Bruyn, J. R. Gelation on the Microscopic Scale. *Phys*. *Rev*. *E* **2008**, *78*, 021405.

(55) Moschakis, T.; Lazaridou, A.; Biliaderis, C. G. Using Particle Tracking to Probe the Local Dynamics of Barley *β*-Glucan Solutions upon Gelation. *J*. *Colloid Interface Sci*. **2012**, *375*, 50−59.

(56) Goodman, A.; Tseng, Y.; Wirtz, D. Effect of Length, Topology, and Concentration on the

Microviscosity and Microheterogeneity of DNA Solutions. *J. Mol. Biol.* **2002**, *323*, 199−215.

(57) Tanaka, F. Thermoreversible Gelation Driven by Coil-to-Helix Transition of Polymers. *Macromolecules* **2003**, *36*, 5392−5405.

(58) Paradossi, G.; Chiessi, E. Tacticity-Dependent Interchain Interactions of Poly(*N*-Isopropylacrylamide) in Water: Toward the Molecular Dynamics Simulation of a Thermoresponsive Microgel. *Gels* **2017**, *3*, 13.

(59) Stryer, L. The Interaction of a Naphthalene Dye with Apomyoglobin and Apohemoglobin. A Fluorescent Probe of Non-Polar Binding Site. *J. Mol. Biol.* **1965**, *13*, 482−495.